Protective Effects of Silymarin Against Photocarcinogenesis in a Mouse Skin Model

*Santosh K. Katiyar, Neil J. Korman, Hasan Mukhtar, Rajesh Agarwal**

Background: **Nonmelanoma skin cancer is the most common cancer among humans; solar UV is its major cause. Therefore, it is important to identify agents that can offer protection against this cancer.** ***Purpose:*** **We evaluated the protective effects of silymarin, a flavonoid compound isolated from the milk thistle plant, against UVB radiation-induced nonmelanoma skin cancer in mice and delineated the mechanism(s) of its action.** ***Methods:*** **For long-term studies, three different protocols of treatment were employed, each evaluating protection by silymarin at a different stage of carcinogenesis. Female SKH-1 hairless mice were subjected to 1) UVB-induced tumor initiation followed by phorbol ester-mediated tumor promotion, 2) 7,12-dimethylbenz[*a*]anthracene-induced tumor initiation followed by UVB-mediated tumor promotion, and 3) UVB-induced complete carcinogenesis. Forty mice were used in each protocol and were divided into control and treatment groups. Silymarin was applied topically at a dose of 9 mg per application before UVB exposure, and its effects on tumor incidence (% of mice with tumors), tumor multiplicity (number of tumors per mouse), and average tumor volume per mouse were evaluated. In short-term studies, the following parameters were measured: formation of sunburn and apoptotic cells, skin edema, epidermal catalase and cyclooxygenase (COX) activities, and enzymatic activity and messenger RNA (mRNA) expression for ornithine decarboxylase (ODC), a frequently observed marker at tumor promotion stage. Fisher's exact test was used to evaluate differences in tumor incidence, two-sample Wilcoxon rank sum test was used for tumor multiplicity and tumor volume, and Student's *t* test was used for all other measurements. All statistical tests were two-sided.** ***Results:*** **In the protocol with UVB-induced tumor initiation, silymarin treatment reduced tumor incidence from 40% to 20% (*P* = .30), tumor multiplicity by 67% (*P* = .10), and tumor volume per mouse by 66% (*P* = .14). In the protocol with UVB-induced tumor promotion, silymarin treatment reduced tumor incidence from 100% to 60% (*P*<.003), tumor multiplicity by 78% (*P*<.0001), and tumor volume per mouse by 90% (*P*<.003). The effect of silymarin was much more profound in the protocol with UVB-induced complete carcinogenesis, where tumor incidence was reduced from 100% to 25% (*P*<.0001), tumor multiplicity by 92% (*P*<.0001), and tumor volume per mouse by 97% (*P*<.0001). In short-term experiments, silymarin application resulted in statistically significant inhibition in UVB-caused sunburn and apoptotic cell formation, skin edema, depletion of catalase activity, and induction of COX and ODC activities and ODC mRNA expression.** ***Conclusions and Implication:*** **Silymarin can provide substantial protection against different stages of UVB-induced carcinogenesis, possibly via its strong antioxidant properties. Clinical testing of its usefulness is warranted. [J Natl Cancer Inst 1997;89:556-65]**

Nonmelanoma skin cancers, composed of basal cell and squamous cell carcinomas, are the most frequently diagnosed cancers in Caucasians and account for almost one million new cases each year in the United States. These skin cancers are caused by excessive exposure to the solar UV radiation (*1-3*). The wavelengths of sunlight most effective in producing nonmelanoma skin cancer lie within UVC (200-290 nm) and UVB (290-320 nm) ranges (*4*). Since ozone in the earth's atmosphere filters out all of the UVC, it has little, if any, biologic relevance to nonmelanoma skin cancer (*5*). Although wavelengths within UVB are the most carcinogenic, animal studies have clearly demonstrated that UVA (320-400 nm) is also capable of producing skin cancer (*6,7*). However, when compared with UVB, UVA-induced skin cancers in mice require much greater exposure and a longer latency period before tumors are evident (*5*). Therefore, in animal studies, UVB is the most frequently used photocarcinogen [reviewed in (*8,9*)]. Because nonmelanoma skin cancer is increasing at an alarming rate, efforts have been made to develop strategies to prevent the deleterious effects of sun exposure. These strategies include avoiding excessive sun exposure by limiting outdoor activities, wearing protective clothing when outside in the sun, and using sunscreens on the body surface that is likely to be exposed to sun; this last strategy has received the most attention (*10*). However, the sunscreen protection can be overwhelmed by excessive length of exposure. In addition, there have been concerns regarding the use of sunscreen and the possible increase in melanoma growth in a mouse model (*11*). The other protection strategy, known as chemoprevention, includes the topical and/or dietary use of chemical agents in an attempt to reduce the risk of nonmelanoma human skin cancer by solar radiation (*12*).

Chemoprevention of cancer is a means of cancer control where the occurrence of the disease, as a consequence of exposure to carcinogenic agents (solar UV for photocarcinogenesis), can be either entirely prevented, slowed, or reversed by administration of one or more chemical agents (*12-15*). It also includes chemotherapy for precancerous lesions, e.g., actinic keratosis in human skin squamous cell carcinomas (*12*). A wide range of

**Affiliations of authors:* S. K. Katiyar (Department of Dermatology), N. J. Korman (Department of Dermatology, University Hospitals of Cleveland), H. Mukhtar, R. Agarwal (Department of Dermatology and Case Western Reserve University Ireland Cancer Center, University Hospitals of Cleveland), Case Western Reserve University, OH.

Correspondence to: Rajesh Agarwal, Ph.D., Department of Dermatology, Case Western Reserve University, 11100 Euclid Ave., Cleveland, OH 44106.

See ''Notes'' following ''References.''

laboratory studies and limited epidemiologic studies in humans have identified many compounds, including several polyphenols, as potential chemopreventive agents against carcinogenesis in various organs (*12-15*). Only limited studies, however, have shown encouraging results regarding chemoprevention against photocarcinogenesis, except for the use of sunscreens. These chemopreventive agents include butylated hydroxytoluene, canthaxanthin, carotenoids, α-difluoromethylornithine, green tea and its major epicatechin constituent, indomethacin, omega-3 fatty acid sources, retinyl palmitate, and vitamin E [reviewed in (*12*)]. Low dietary fat (*16*), retinoids [reviewed in (*17*)], and indomethacin (*18*) have also been shown to reduce nonmelanoma skin cancer development in human population.

UVB can exert its biologic effect only after it is absorbed by a chromophore (a molecule with structural features that allow absorption of light) in the skin (*19*). UVB can cause alterations in DNA structure directly or it can be absorbed by other cellular molecules, such as lipids in the membranes generating reactive oxidative moieties, causing DNA damage and lipid peroxidation reactions that trigger the cell-signaling pathways leading to gene activation [reviewed in (*19*)]. Because UV radiation of certain wavelengths can cause skin cancer (*4*) as well as DNA damage (*20,21*), it is agreed that DNA is one chromophore for UVB (*19-21*). UVB is strongly absorbed by cellular DNA in skin and results in several different types of DNA damage; cyclobutane pyrimidine dimers and 6-4 photoproducts are the most important with respect to photocarcinogenesis (*22-24*). In addition, oxidative stress involving generation of free radicals and reactive oxygen species (ROS) and a depletion of antioxidant machinery in removing these moieties are also important consequences of UVB exposure to mammalian skin. These oxidative reactions can also lead to DNA damage and to several other biochemical and molecular events that ultimately lead to tumorigenesis [reviewed in (*25-29*)]. Therefore, agents that could protect UVB-caused cellular DNA damage and/or possess strong antioxidant properties may be useful against photocarcinogenesis. An ideal agent against photocarcinogenesis should be able to penetrate the skin and be able to protect against UVB radiation-induced injury caused by oxidative reactions.

For the past two decades, silymarin (2-[2,3-dihydro-2-(4-hydroxy-3-methoxyphenyl)-3-(hydroxymethyl)-1,4-benzodioxin-6-yl]-2,3-dihydro-3,5,7-trihydroxy-4*H*-1-benzopyran-4-one; Fig. 1), a flavonoid compound isolated from milk thistle plant (*Silybum marianum* (*L.*) *Gaertn*) (artichoke is one of the members in this family) has been used clinically in Europe as an antihepatotoxic agent (*30-32*). Mechanistic studies (*33,34*) have shown that silymarin is a very strong antioxidant compound capable of scavenging both free radicals and ROS, and thus it increases the antioxidant potential of cells by ameliorating the deleterious effects of free radical reactions. Furthermore, an increase in ornithine decarboxylase (ODC) activity in epidermis is a prerequisite (but not obligatory step) for skin tumor promotion (*35-37*). We have shown that silymarin possesses strong inhibitory effects against the induction of epidermal ODC activity and messenger RNA (mRNA) expression in SENCAR mice caused by 12-*O*-tetradecanoylphorbol-13-acetate (TPA) and several other known tumor promoters (*38*). This suggested that silymarin could also be a useful agent against UVB-induced changes.

In the present study, we assessed the protective effects of silymarin against photocarcinogenesis in the SKH-1 hairless mouse skin model. In this model, UVB was used both as a tumor initiator and as a tumor promoter as well as a complete carcinogen [reviewed in (*12*)]. The rationale for the selection of these three protocols was to dissect out the protective effects of silymarin at different stages of photocarcinogenesis, i.e., 1) UVB-induced tumor initiation stage, 2) UVB-induced tumor promotion stage, or 3) UVB-induced tumor initiation and tumor promotion (UVB-induced complete carcinogenesis). On the basis of long-term tumorigenesis results, additional studies were also performed to delineate the mechanism(s) of protection imparted by silymarin.

Materials and Methods

Animals and UVB Light Source

Female SKH-1 hairless mice (6 weeks old) obtained from Charles River Laboratories (Wilmington, MA) were used in this study. After their arrival in the animal facility, the animals were allowed to acclimatize for 15 days before the start of the experiments and were fed Purina Chow diet and water ad libitum. Throughout the experimental protocols, the mice were maintained at standard conditions: temperature of 24 ± 2 °C, relative humidity of 50% ± 10%, and 12-hour room light/12-hour dark cycle. For UVB irradiation, the mice were housed in specially designed cages where they were held in dividers separated by Plexiglas. The distance between light source to target skin was 23 cm in all of the UVB irradiations (*39*). The UVB light source used was a bank of four Westinghouse FS-40-T-12 fluorescent sunlamps equipped with a UVB Spectra 305 Dosimeter (Daavlin Co., Bryan, OH). This light source emitted about 80% radiation in the range of 280-340 nm, with peak emission at 314 nm as monitored with an SEE 240 photodetector, 103 filter, and 1008 diffuser attached to an IL 700 Research Radiometer (International Light, Newburyport, MA).

Long-term Photocarcinogenesis Studies

Three different long-term tumorigenesis protocols were employed to assess the protective effect of silymarin against 1) UVB-induced tumor initiation, 2) UVB-induced tumor promotion, and 3) UVB-induced complete carcinogenesis (both tumor initiation and tumor promotion caused by UVB radiation) as detailed by Wang et al. (*40*). These protocols are summarized schematically in Fig. 2.

For the studies involving blocking of UVB-caused tumor initiation by silymarin, the mice were divided into two groups of 20 each and treated with either 200 μL acetone alone (control group) or 9 mg silymarin (Aldrich Chemical Co., Milwaukee, WI) in 200 μL acetone (treated group) per mouse per day. These treatments were continued daily for 14 days. On the 15th day, mice in both groups began to receive UVB irradiation at a dose of 180 mJ/cm^2 per day. The UVB irradiation was continued daily for 10 days; therefore, the total UVB dose used was 1800 mJ/cm^2 fractionated in 10 equal doses for 10 days. One week after the last UVB exposure, animals in both groups were treated topically with 10 nmol (6.17 ng) of TPA as tumor promoter (Sigma Chemical Co., St. Louis, MO) in 200 μL acetone per mouse per application. The TPA treatment was given twice a week up to the end of the experiment at 30 weeks following the last UVB exposure.

For the studies involving blocking of UVB-caused tumor promotion by silymarin, the mice were divided into two groups of 20 animals each and were

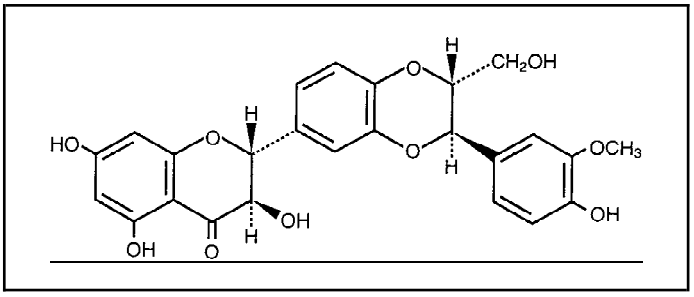

Fig. 1. Chemical structure of silymarin.

treated topically with a single application of 200 nmol (51.2 μg) of 7,12-dimethylbenz[*a*]anthracene (DMBA) (Aldrich Chemical Co.) in 200 μL acetone per mouse. One week following tumor initiation with DMBA, the mice were treated with 200 μL of acetone alone (control group) or 9 mg silymarin in 200 μL of acetone (treated group) per mouse. Thirty minutes later, the mice in both groups were irradiated with a 180-mJ/cm^2 dose of UVB. The acetone or silymarin treatment followed by UVB exposure was conferred twice a week until the end of the experiment at 30 weeks from the start of the UVB exposure.

For the studies involving blocking of UVB-caused complete carcinogenesis by silymarin, the mice were divided into two groups of 20 animals each and treated with either 200 μL acetone alone (control group) or 9 mg silymarin in 200 μL acetone (treated group) per mouse per day. These treatments were continued daily for 14 days, and on the 15th day the mice in both groups were irradiated with a 180-mJ/cm^2 dose of UVB. The UVB irradiation was continued daily for 10 days; therefore, the total UVB dose used was 1800 mJ/cm^2 fractionated in 10 equal doses for 10 days. One week after the last UVB exposure, the mice were treated either with 200 μL acetone alone (control group) or 9 mg silymarin in 200 μL acetone (treated group) per mouse. Thirty minutes after these treatments, the mice in both groups were irradiated with a 180-mJ/cm^2 dose of UVB. The acetone or silymarin treatment followed by UVB exposure was conferred twice a week until the end of the experiment at 30 weeks from the last UVB exposure as tumor initiator.

Animals in all three protocols were monitored for food and water consumption and any apparent signs of toxicity, such as weight loss or mortality, during the entire study period. Skin tumor formation, as evidenced by an outgrowth greater than 1 mm in diameter and persisting for 2 or more weeks, was recorded. Tumor incidence and multiplicity were recorded weekly until the 30th week in all three protocols. At the end of the 30th week, the dimensions of all of the tumors on the back of each mouse were also recorded, and the tumor volumes were calculated by the hemiellipsoid model formula: tumor volume = 1/2 $(4\pi/3) \times (l/2) \times (w/2) \times h$, where l = length, w = width, and h = height.

Short-term Studies Evaluating Cellular, Biochemical, and Molecular Events

Female SKH-1 hairless mice (Charles River Laboratories), maintained as described above, were divided into five groups of four animals each. The mice in the first group received a topical application of 200 μL acetone alone, and those in the second group received 9 mg silymarin in 200 μL acetone per mouse. Thirty minutes after these treatments, the mice in both of these groups were exposed to UVB at a dose of either 180 or 900 mJ/cm^2. The mice in the third group were left untreated, whereas the fourth group of mice received 9 mg silymarin in 200 μL acetone topically without any UVB radiation. The mice in the fifth group were exposed to UVB at a dose of 900 mJ/cm^2, and, immediately following UVB irradiation, they received 9 mg silymarin topically in 200 μL acetone per mouse. The following parameters were measured at 24 and/or 48 hours after UVB exposure: 1) sunburn and apoptotic cell formation, 2) skin edema, 3) epidermal enzyme activities, such as catalase, cyclooxygenase (COX), and ODC, and 4) ODC mRNA expression.

Sunburn and apoptotic cell formation. Twenty-four hours after UVB exposure at a dose of 900 mJ/cm^2, all of the mice in each group were killed, and the dorsal skin of each mouse was excised, fixed in 10% buffered formalin, and embedded in paraffin. Vertical sections of the skin (5 μm thick) were cut, mounted on glass slides, and stained with hematoxylin–eosin (H & E). Each

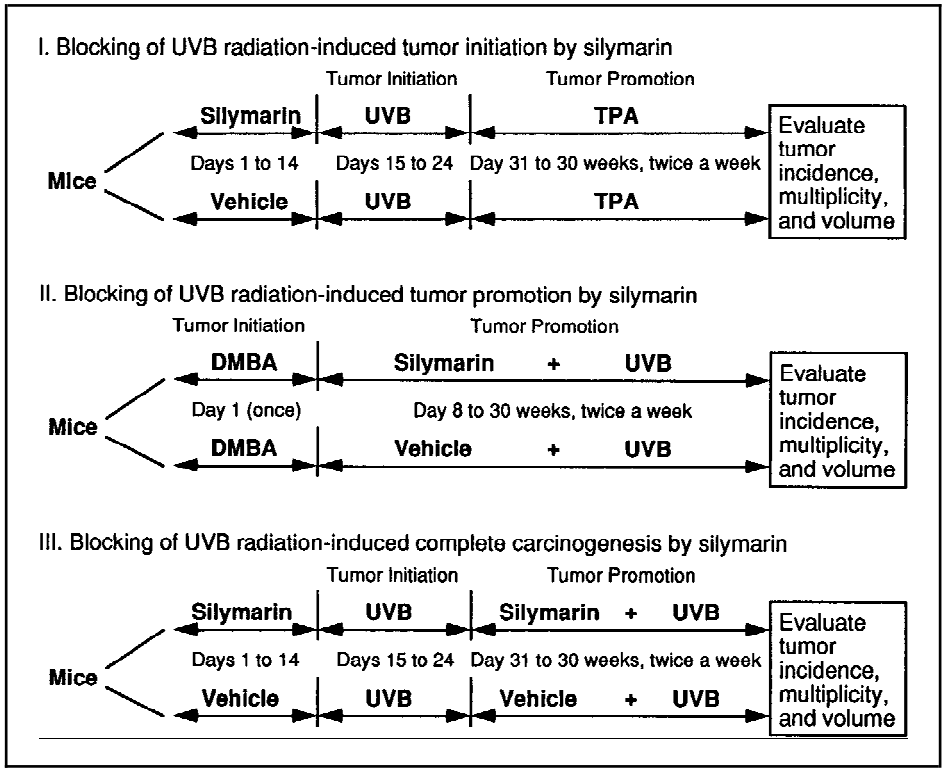

Fig. 2. Schematic presentation of long-term treatment protocols used to assess the protective effect of silymarin at different stages of photocarcinogenesis. Forty female SKH-1 hairless mice were used in each protocol and were divided into control and treatment groups, with 20 animals in each. In studies evaluating the blocking of UVB radiation-induced tumor initiation, silymarin was applied at the dose of 9 mg (dissolved in 200 μL acetone) per application per mouse per day for 14 consecutive days (days 1-14). Control group of mice received 200 μL acetone per application per mouse per day during this period. To achieve UVB radiation-induced tumor initiation, beginning on day 15, animals in both of the groups were exposed to UVB radiation at the dose of 180 mJ/cm^2 per day for 10 continuous days (days 15-24). One week after last UVB exposure (day 31), animals in both of the groups were treated topically with 6.17 ng of 12-*O*-tetradecanoylphorbol-13-acetate (TPA) dissolved in 200 μL acetone per mouse per application to achieve tumor promotion. The TPA application was performed twice a week up to 30 weeks from the last UVB exposure. In studies evaluating the blocking of UVB radiation-induced tumor promotion by silymarin, the mice in both the control and treatment groups were treated topically once with 51.2 μg of 7,12-dimethylbenz[*a*]anthracene (DMBA) dissolved in 200 μL acetone per mouse to achieve tumor initiation. One week later (day 8), animals in the treatment group were applied topically with silymarin at the dose of 9 mg (dissolved in 200 μL acetone) per application per mouse per day. Control group of animals received 200 μL acetone per application per mouse per day. Thirty minutes later, the animals in both of the groups were exposed to UVB radiation at the dose of 180 mJ/cm^2 per day to achieve UVB radiation-induced tumor promotion. The silymarin or vehicle treatments followed by UVB irradiation were performed twice a week up to 30 weeks from the start of UVB exposure. In studies evaluating the blocking of UVB-induced complete carcinogenesis by silymarin, a combination of UVB radiation-induced tumor initiation and tumor-promotion protocols described above was used. Briefly, silymarin was applied at the dose of 9 mg per application for 14 days (days 1-14) in the treatment group, and the control animals received the vehicle during this period. To achieve UVB radiation-induced tumor initiation, beginning on day 15 animals in both of the groups were exposed to UVB radiation at the dose of 180 mJ/cm^2 per day for 10 days (days 15-24). One week after the last UVB exposure (day 31), animals in the treatment group received silymarin topically at the dose of 9 mg per application, whereas the control group of animals received the vehicle. Thirty minutes later, the animals in both of the groups were exposed to UVB radiation at the dose of 180 mJ/cm^2 to achieve UVB radiation-induced tumor promotion. The silymarin or vehicle treatments followed by UVB irradiation were performed twice a week up to 30 weeks from the last UVB exposure as tumor initiator. In each protocol, animals were evaluated for tumor incidence and multiplicity throughout the experiment and for tumor volume at the end of 30 weeks.

section was examined under light microscopy for the formation of sunburn cells by the same individual in a blinded manner. Sunburn cells were scored as eosinophilic cells with pyknotic nuclei or without nuclei and were counted in the interfollicular epidermis (*41*). A total of 64 fields (16 fields per skin section per sample, a total of four skin samples from four mice) were examined per group. Apoptotic cells within the total sunburn cell population were identified by in situ end-labeling of fragmented nuclear DNA by terminal deoxynucleotidyl transferase (TdT). The ApopTag in situ detection kit (Oncor, Gaithersburg, MD) that uses direct immunoperoxidase detection of digoxigenin-labeled genomic DNA was employed. The labeling target was the multitude of new 3′-hydroxy DNA ends generated by DNA fragmentation and typically localized in cells with morphologically identifiable nuclei. Cytoplasmic positivity of apoptotic cells reflected leakage of the small DNA fragments from the nucleus. The paraffin-embedded skin tissue sections from different groups of SKH-1 hairless mice were subjected to a protocol provided by the vendor. With each tissue section, a negative-stained control (using buffer in place of TdT enzyme) was also run to facilitate the identification of apoptotic bodies. The TdT enzyme-mediated end-labeling of the nuclear DNA was detected by a diaminobenzidine reagent with methyl green as counter stain.

Skin edema. To assess the UVB-caused skin edema and the protective effect of silymarin, increase in bifold skin thickness and ear-punch weight were measured at 24 and 48 hours after UVB irradiation at a dose of 900 mJ/cm^2. The increase in bifold skin thickness, as measured by micrometer, was calculated by subtracting the values for the untreated control animals (silymarin untreated and no UVB exposure) from those for the treated animals (UVB exposed or silymarin treated and UVB exposed). At least eight determinations were made at different dorsal skin sites per mouse in each group. For increase in ear-punch weight studies, an identical protocol was employed, except that silymarin (0.45 mg dissolved in 10 μL acetone per side of ear) was applied topically on both sides of each ear. A 4-mm-diameter punch of ear skin through the entire ear (four from each ear of the same mouse) was taken and quickly weighed. An increase in the amount of fluid following UVB exposure was calculated by subtracting the values for the untreated controls from those for the treated animals. Each determination included a total of eight ear-punch biopsy specimens per mouse in each group.

Enzyme activities. Twenty-four hours after UVB exposure at a dose of 180 or 900 mJ/cm^2, the mice were killed, the dorsal skin of each mouse was excised, the epidermis was separated, and 100 000*g* epidermal cytosolic and microsomal fractions were prepared (*39*). Catalase activity was determined in cytosol by following the decomposition of hydrogen peroxide (H_2O_2) measured as a decrease in absorbance at 240 nm as described previously (*39*) and expressed as nanomoles H_2O_2 consumed per minute per milligram protein. COX activity was determined in microsomes by measuring the formation of prostaglandin (PG) metabolites from [^{14}C]arachidonic acid as described previously (*39*) and expressed as picomoles PGE_2, $PGF_{2\alpha}$, and PGD_2 metabolite formed per 15 minutes per milligram protein. ODC activity was determined in cytosol by measuring the release of $^{14}CO_2$ from the *d,l*-[^{14}C]ornithine as described previously (*38*,*39*) and expressed as picomoles CO_2 released per hour per milligram protein.

ODC mRNA expression. Twenty-four hours after UVB exposure at a dose of 900 mJ/cm^2, the mice were killed, the dorsal skin of each mouse was excised, the epidermis was separated, and the total epidermal RNA was isolated by CsCl gradient (*38*). The RNA pellets were resuspended in Tris–EDTA buffer (pH 7.5), and poly(A)$^+$ RNA was isolated from total RNA with the use of QuickPrep mRNA Purification Kit (Pharmacia Biotech Inc., Piscataway, NJ) as per the vendor's protocol. Northern blot analysis using poly(A)$^+$ RNA was performed as described earlier (*38*). In brief, 4 μg poly(A)$^+$ RNA for each sample was dried and the pellet was dissolved in 10 μL denaturing buffer (5 μL formaldehyde, 2 μL formamide, 1 μL 10× MOPS buffer [0.4 *M* MOPS {3-(*N*-Morpholino)-propanesulfonic acid}, 0.1 *M* sodium acetate, and 10 m*M* EDTA; pH 7.0], and 2 μL water) plus 1 μL ethidium bromide. The samples were heated for 10 minutes at 65 °C, chilled on ice, and then electrophoresed through a 1.2% agarose gel (wt/vol) containing 6.6% formaldehyde (vol/vol) in 1× MOPS buffer. Fractionated RNA was transferred by capillary action to Nytran membrane for 6 hours employing 10× standard saline citrate (SSC) (1.5 *M* sodium chloride and 150 m*M* sodium citrate, pH 7.0) as the transfer buffer. The membrane was air-dried and heated in a vacuum for 2 hours at 80 °C. Prehybridization of the membrane was performed for 2 hours at 42 °C in the prehybridization buffer (50% deionized formamide, 5% Denhardt's solution [2% bovine serum albumin, 2% Ficoll, and 2% polyvinylpyrrolidone], 10% sonicated salmon sperm DNA [2 mg/mL], 5% sodium dodecyl sulfate [SDS], 25% 20× SSC buffer, and 10% dextran sulfate). The ^{32}P-labeled probe for ODC mRNA was generated with a random primed labeling kit (USB Corp., Cleveland, OH). The substrate was an ODC complementary DNA (cDNA) fragment of about 2.1 kilobase that was purified from plasmid pOD48 (from Dr. Ajit K. Verma, University of Wisconsin Comprehensive Cancer Center, Madison). The labeled ODC probe was denatured and then added directly to the prehybridization buffer (1×10^6 dpm/mL). The membrane was hybridized overnight at 42 °C and then washed twice in 6× SSC containing 0.5% SDS followed by one washing in 1× SSC containing 0.1% SDS for 15 minutes. The final wash was carried out in 1× SSC with 0.1% SDS for 30 minutes at 56 °C. The membrane was then exposed to x-ray film (XAR-5) with intensifying screens at −70 °C.

Statistical Analysis

In long-term tumorigenesis experiments, the statistical significance of difference between the tumor incidence in silymarin-treated and untreated groups was determined by two-tailed Fisher's exact test by use of the StatXact version 3 program (Cytel Software Corporation, Cambridge, MA). For tumor multiplicity and tumor volume per mouse, a two-sample Wilcoxon rank sum test was employed. An advantage of the Wilcoxon rank sum test is that its validity does not depend on any assumption about the shape of the distribution of tumor multiplicities. For all of the measurements performed in short-term studies, a two-tailed Student's *t* test was used to assess the statistical significance of the difference between treated and untreated groups.

Results

Protective Effect of Silymarin Against Photocarcinogenesis: Long-term Studies

Topical application of silymarin prior to UVB irradiation resulted in a substantial protection against photocarcinogenesis in the SKH-1 hairless mouse skin model (Fig. 3). In studies involving protection at tumor initiation stage, as shown in Fig. 3, A and B, application of silymarin for 14 days before UVB exposure resulted in a reduction in both the percentage of mice with tumors and the number of tumors per mouse in silymarin-treated animals compared with the vehicle-treated controls. This was evident during the entire treatment period. At the end of the experiment at 30 weeks, the animals in the silymarin-treated group showed a 20% reduction in tumor incidence compared with vehicle-treated control animals, ($P = .30$; tumor incidence = 0.2 and 95% confidence interval [CI] = 0.057-0.436 for silymarin-treated group; and tumor incidence = 0.4 and 95% CI = 0.19-0.64 for vehicle-treated control group) (Fig. 3, A) and a 67% reduction in tumor multiplicity ($P = .10$) (Fig. 3, B). These differences were not statistically significant. At the end of 30 weeks, the tumor volume per mouse in the silymarin-treated group showed a 66% reduction ($P = .14$) compared with the vehicle-treated control group (3.4 ± 2.5 [mean ± standard error] mm^3 per mouse versus 10.1 ± 5.8 [mean ± standard error] mm^3 per mouse). These differences were also not statistically significant.

In studies assessing the protective effect of silymarin during tumor promotion stage, as shown in Fig. 3, C and D, its application prior to each UVB exposure resulted in an extended latency period by an additional 3 weeks before the onset of the first tumor and reduced tumor incidence and multiplicity throughout the treatment period. At the termination of the experiment, the animals in the silymarin-treated group showed a 40% reduction in tumor incidence ($P<.003$; tumor incidence = 0.6 and 95% CI = 0.36-0.81 for the silymarin-treated group; and tumor incidence = 1 and 95% CI = 0.86-1 for the vehicle-

treated control group) (Fig. 3, C) and a 78% reduction in tumor multiplicity ($P<.0001$) (Fig. 3, D). The vehicle-treated control group showed a tumor volume of 174.7 ± 119.1 mm^3 per mouse compared with only 16.5 ± 7.3 mm^3 per mouse after silymarin treatment. The silymarin treatment thus accounts for a highly significant reduction (90%; $P<.003$).

A much more profound protective effect of silymarin was observed in studies involving complete carcinogenesis by UVB. As shown in Fig. 3, E and F, application of silymarin for 14 days prior to UVB exposure as a tumor initiator and then again during UVB-induced tumor promotion resulted in a delay of latency period by 9 weeks and afforded highly significant protection in terms of both tumor incidence and tumor multiplicity throughout the treatment period. At the end of the experiment, 100% of the mice in the vehicle-treated control group had tumors, whereas only 25% of the mice had tumors after silymarin treatment. This accounted for a 75% protection in tumor incidence ($P<.0001$, tumor incidence = 0.25 and 95% CI = 0.087-0.49 for the silymarin-treated group; and tumor incidence = 1 and 95% CI = 0.86-1 for the vehicle-treated control group) (Fig. 3, E). In terms of tumor multiplicity, silymarin treatment resulted in a 92% reduction ($P<.0001$) in number of tumors per mouse (Fig. 3, F). Similar to the experiments involving protection only at the tumor promotion stage, silymarin treatment in this protocol also showed a significant reduction (97%; $P<.0001$) in the tumor volume per mouse (84.0 ± 21.9 mm^3 per mouse in the vehicle-treated control animals versus only 2.4 ± 1.1 mm^3 per mouse in the silymarin-treated animals). No signs of toxicity, body weight loss, or mortality were observed following silymarin treatment in all three protocols.

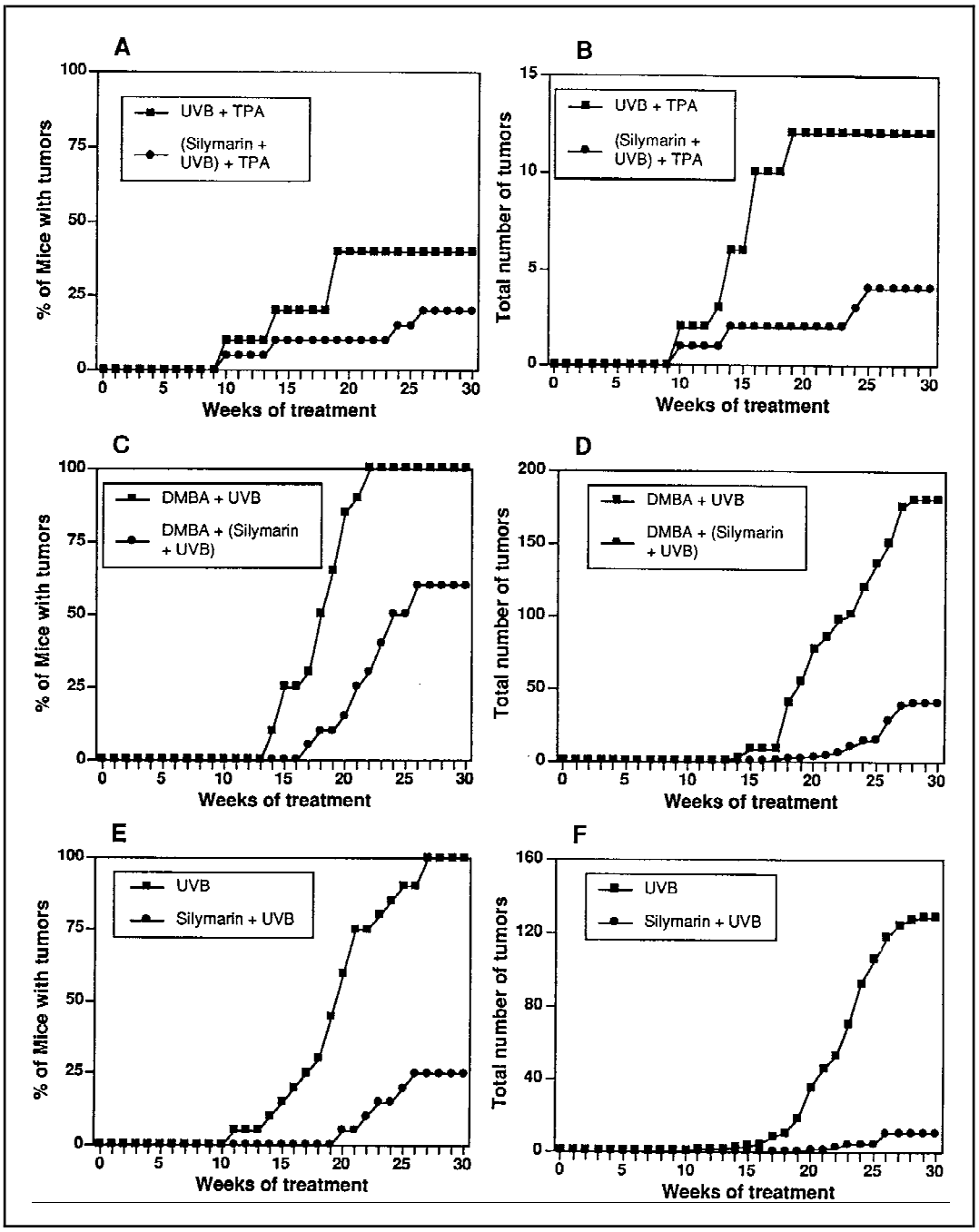

Fig. 3. Protective effects of silymarin against UVB radiation-induced tumor initiation (panels **A** and **B**), tumor promotion (**C** and **D**), and complete carcinogenesis (**E** and **F**) in SKH-1 hairless mouse skin. The details of all three experimental protocols are described in the ''Materials and Methods'' section and summarized schematically in Fig. 2. The percentages of mice with tumors (left panels) and total number of tumors per mouse (right panels) were plotted as a function of the number of weeks of treatment. The data from 20 mice per group are shown.

Inhibitory Effect of Silymarin on UVB-Caused Sunburn Cell and Apoptotic Cell Formation

We assessed the effect of preapplication of silymarin on UVB-induced formation of sunburn cells and apoptotic cells in SKH-1 hairless mouse epidermis. As observed by histologic evaluation, silymarin treatment resulted in a highly significant reduction in the number of sunburn cells and apoptotic cells after UVB exposure (Fig. 4). When stained with H & E, compared with controls (Fig. 4, left panel A), the UVB-irradiated skin sections showed the cells with the classic appearance of sunburn cells: pyknotic nuclei, chromatin condensation, and intensely eosinophilic cytoplasm (Fig. 4, left panel B). Preapplication of silymarin, however, showed a highly significant reduction in UVB-induced sunburn cell formation (Fig. 4, left panel C). The skin sections of the control animals (no UVB) showed only 3.8 ± 0.9 sunburn cells per cm of epidermis and UVB irradiation of skin resulted in 165.5 ± 15.8 sunburn cells/cm of epidermis. However, with silymarin treatment prior to UVB, only 37.7 ± 2.2 sunburn cells per cm of epidermis were scored. This accounted for a 77% inhibition ($P<.001$) by silymarin.

When tissue sections were stained employing an ApopTag in situ kit, apoptotic cells were observed only in skin sections of UVB-exposed mice (Fig. 4, right panel B). As evident by the specific brown staining by diaminobenzidine reaction, the apoptotic cells showed pyknotic nuclei, chromatin condensation, and degradation (Fig. 4, right panel B). No apoptotic cells, however, were observed in the skin sections of either unirradiated (Fig. 4, right panel A) or silymarin-pretreated UVB-irradiated (Fig. 4, right panel C) mice.

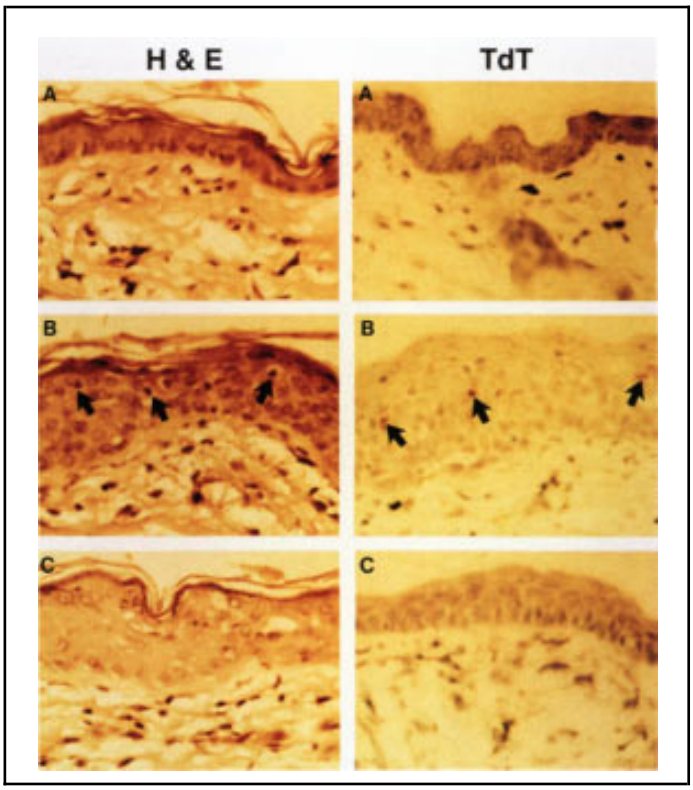

Fig. 4. Inhibitory effect of silymarin on UVB-caused sunburn cell (left panels) and apoptotic cell (right panels) formation in SKH-1 hairless mice. The groups of mice (four animals per group) were either unexposed, exposed to UVB radiation (900 mJ/cm^2), or topically treated with silymarin (9 mg in 200 μL acetone per mouse) on dorsal skin and then 30 minutes later exposed to the same dose of UVB. The hematoxylin and eosin and ApopTag terminal deoxynucleotidyl transferase immunohistochemical stainings were performed on tissue sections as detailed in the ''Materials and Methods'' section. **A)** untreated skin (no UVB exposure); **B)** UVB-irradiated skin; and **C)** silymarin-pretreated UVB-irradiated skin. Arrows in the left panel show sunburn cells and in the right panel show apoptotic cells with brown staining. Original magnification ×40.

Inhibitory Effect of Silymarin on UVB-Caused Cutaneous Edema

We have shown previously (*39*) that a single UVB exposure of SKH-1 hairless mice at a 900-mJ/cm^2 dose results in a significant cutaneous edema up to 48 hours after irradiation. Therefore, its inhibition by silymarin was evaluated at both 24 and 48 hours. In terms of an increase in bifold skin thickness over untreated controls, as shown in Fig. 5, A, application of silymarin prior to UVB irradiation resulted in 44% and 51% inhibition ($P<.001$ for both) in UVB-induced cutaneous edema at 24 and 48 hours, respectively. When silymarin was applied topically immediately after UVB irradiation, it showed comparable inhibitory effect (42% and 54% inhibition; $P<.001$ for both) to that prior to UVB (Fig. 5, A). Treatment of mice with silymarin alone (no UVB exposure) did not result in an increase in bifold skin thickness. As measured by an increase in ear-punch weight over untreated control animals, preapplication of silymarin onto the ear skin also showed a comparable inhibitory effect against UVB-induced ear edema at both 24 hours (49% inhibition; $P<.001$) and 48 hours (45% inhibition; $P<.001$) after irradiation (Fig. 5, B).

Inhibitory Effect of Silymarin on UVB-Caused Depletion of Epidermal Catalase Activity

In these studies, while epidermis from untreated control mice showed catalase enzyme activity of 506 ± 26 U (nanomoles of H_2O_2 consumed per minute per milligram protein), irradiation of mice once with a 900-mJ/cm^2 dose of UVB radiation resulted in enzyme activity of 280 ± 10 U, thus accounting for a 45% depletion in epidermal catalase activity 24 hours after irradiation. However, application of silymarin at a dose of 9 mg prior to UVB irradiation showed enzyme activity of 365 ± 16 U that indicated much less (28%) depletion in enzyme activity compared with that after UVB exposure alone.

Inhibitory Effect of Silymarin on UVB-Caused Induction of Epidermal COX and ODC Activities and ODC mRNA Expression

The formation of PGE_2, $PGF_{2\alpha}$, and PGD_2 was quantitated in mouse epidermis after the irradiation of animals at UVB doses of 180 or 900 mJ/cm^2. An increase in epidermal COX activity at 24 hours after irradiation (Fig. 6) was observed, as seen by an increase in PGE_2 and PGD_2 levels at both doses of UVB; a significant increase in $PGF_{2\alpha}$ formation was observed, only after the 900-mJ/cm^2 UVB dose. The increase in epidermal COX activity as measured by formation of all these PG metabolites was more profound at the 900-mJ/cm^2 UVB dose than at the 180-mJ/cm^2 dose (Fig. 6). Topical application of silymarin prior to UVB irradiation, however, resulted in a highly significant inhibition of UVB-caused induction of epidermal COX activity

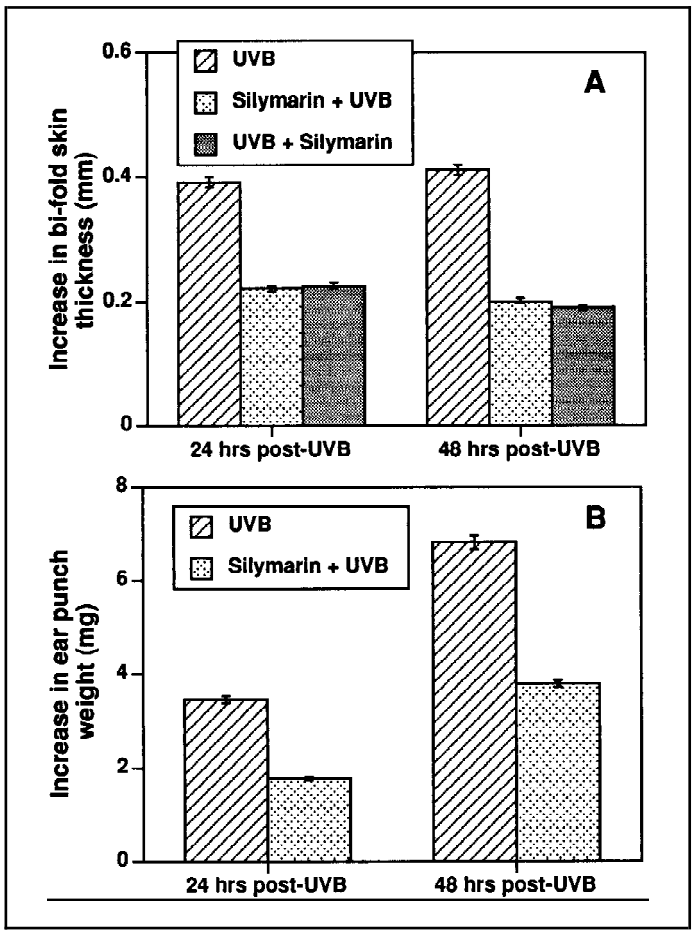

Fig. 5. Inhibitory effect of silymarin on UVB-caused edema in SKH-1 hairless mice. For skin edema studies, the groups of mice (four animals per group) were 1) unexposed (untreated control), 2) treated topically on dorsal skin with silymarin (9 mg in 200 μL acetone per mouse), 3) exposed to UVB radiation (900 mJ/cm^2), 4) treated topically on dorsal skin with silymarin (9 mg in 200 μL acetone per mouse) and then 30 minutes later exposed to UVB radiation (900 mJ/cm^2), or 5) first exposed to UVB radiation (900 mJ/cm^2) and immediately thereafter treated topically with silymarin (9 mg in 200 μL acetone per mouse). In case of ear skin edema studies, an identical protocol was used, except that instead of the dorsal skin, silymarin was applied topically on both sides of each ear (0.45 mg in 10 μL acetone per side of the ear) only prior to UVB exposure. Twenty-four and 48 hours after UVB irradiation, the dorsal skin **(A)** and ear skin **(B)** edema were determined by measuring the bifold skin thickness of the exposed dorsal skin and by weighing the ear-punch (4 mm each) biopsy specimens, respectively. In each case, the data shown are after subtraction of the values for unexposed controls. **A)** The dorsal skin edema was measured as an increase in bifold skin thickness following UVB exposure and represents mean ± standard error (SE) of four mice; at least eight determinations were made at different skin sites for every animal. **B)** The ear skin edema was measured as an increase in ear-punch weight following UVB exposure and represents the mean ± SE of four mice; eight ear-punch biopsy specimens (four from each ear) were pooled as one determination per animal.

(Fig. 6). Silymarin treatment prior to UVB exposure (at both doses) resulted in 95% (P<.001) and 66% (P<.001) inhibition, respectively, in the induction of PGE_2 formation by UVB (Fig. 6). For $PGF_{2\alpha}$ and PGD_2 metabolites, the inhibitory effect of silymarin ranged between 31% (P<.01) and 67% (P<.001) (Fig. 6). Similarly, when silymarin was applied topically at 9 mg per dose immediately after UVB exposure at the dose of 900 mJ/cm^2, it showed significant inhibition (P<.001 for PGE_2 and P<.01 for $PGF_{2\alpha}$ and PGD_2) in the induction of all three PG metabolites' formation by UVB (Fig. 6). Silymarin alone at a dose of 9 mg per mouse did not cause an increase in epidermal COX activity (Fig. 6).

Irradiation of mice with a 180- or 900-mJ/cm^2 UVB dose also resulted in a highly significant increase (~10- and 26-fold, respectively) in epidermal ODC activity (Fig. 7) 24 hours after irradiation; the basal epidermal ODC activity in unexposed mice was 44 ± 5 pmol/hr per mg protein. However, application of silymarin prior to UVB exposure (at both doses) resulted in 97% (P<.0001) and 64% (P<.001) inhibition, respectively, of UVB-induced epidermal ODC activity (Fig. 7). Similarly, application of silymarin immediately after UVB exposure at the 900-mJ/cm^2 dose also resulted in significant (P<.001) inhibition (60%) of UVB-induced epidermal ODC activity (Fig. 7). Silymarin alone at a dose of 9 mg per mouse did not cause an increase in epidermal ODC activity (Fig. 7). Since UVB-induced ODC activity in mouse skin is due to an increase in the ODC mRNA level (*42*), studies were also performed to determine if UVB-induced mRNA synthesis in epidermis is influenced by preapplication of silymarin. When total RNA samples were analyzed, no ODC mRNA expression was observed, even in the UVB-irradiated epidermis (data not shown). Additional studies, therefore, were performed employing poly(A)$^+$ RNA samples. As shown in Fig. 8, compared with untreated control (lane 1) showing a very faint band accounting for negligible ODC mRNA expression, exposure of mice with the 900-mJ/cm^2 UVB dose (lane 2) resulted in a highly statistically significant increase in the expression of epidermal ODC mRNA 24 hours after irradiation. However, ODC mRNA expression in the epidermis from UVB-irradiated mice (Fig. 8) was highly elevated compared with that from silymarin-pretreated and UVB-irradiated mice (Fig. 8). These results show that silymarin treatment results in a highly significant inhibition of UVB-caused increase in ODC mRNA expression in the epidermis. The reprobing of stripped northern blot with glyceraldehyde-3-phosphate dehydrogenase showed equal loading of poly(A)$^+$ RNA samples in each case. The mice treated with silymarin alone at the dose of 9 mg per mouse showed no signs of toxic effects on the skin, such as irritation and inflammation.

Discussion

The central finding in this study is that silymarin, a naturally occurring flavonoid, affords substantial protection against photocarcinogenesis in a mouse model. This effect of silymarin is due to inhibition of several different events associated with UVB-induced tumor initiation and tumor promotion. In studies assessing the protection against UVB radiation-induced tumor initiation, silymarin showed considerable reduction in tumor incidence, tumor multiplicity, and tumor volume per mouse. None of these reductions, however, were statistically significant, possibly because of low tumor incidence and multiplicity in the UVB-alone control group. This may be because the dose and the exposure regimen of UVB radiation used were not sufficient for strong tumor initiation. Conversely, when UVB radiation was used as both tumor initiator and tumor promoter (complete carcinogenesis protocol), 100% of the animals showed tumor incidence, with a total of 128 tumors. In this protocol, although UVB exposures were dissected to achieve tumor initiation and tumor promotion, UVB exposure during promotion could also

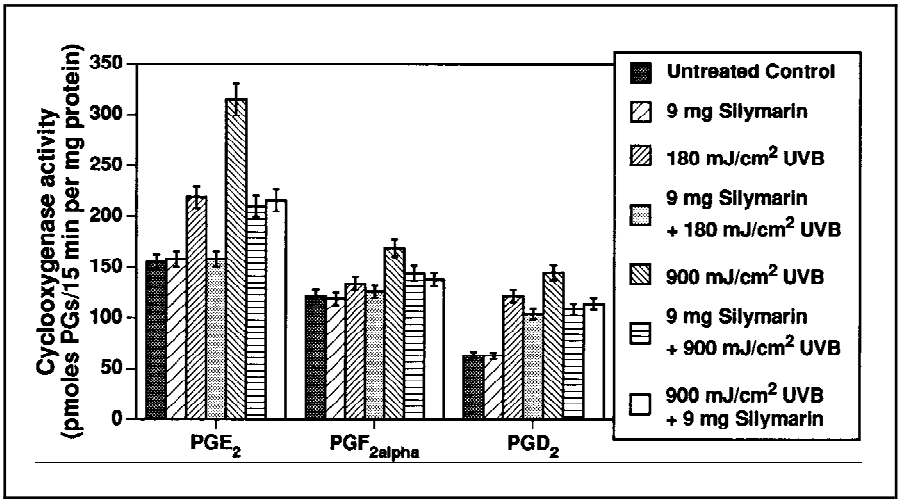

Fig. 6. Inhibitory effect of silymarin on UVB-caused induction of epidermal cyclooxygenase (COX) activity in SKH-1 hairless mice. The groups of mice (four animals per group) were either unexposed (untreated control), treated topically on dorsal skin with silymarin (9 mg in 200 μL acetone per mouse), exposed to UVB radiation (180 mJ or 900 mJ/cm^2), with or without topical application of silymarin (9 mg in 200 μL acetone per mouse) 30 minutes prior to UVB radiation, or first exposed to UVB radiation (900 mJ/cm^2) and immediately thereafter treated topically with silymarin (9 mg in 200 μL acetone per mouse). Twenty-four hours after UVB irradiation, the animals were killed, the epidermal cytosolic fraction was prepared, and COX activity was determined. The data shown as COX activity (picomoles prostaglandins [PGs] per 15 minutes per milligram protein) are mean ± standard error of four mice; each assay was performed in duplicate.

have resulted in additional tumor initiation leading to high tumorigenicity. This is consistent with the studies reported earlier (*8,9,43*). When the protective effect of silymarin was observed in this protocol, it showed statistically significant ($P<.0001$) reduction in tumor incidence, tumor multiplicity, and tumor volume per mouse. The protective effect of silymarin was also statistically significant when assessed in a UVB radiation-induced tumor promotion protocol. Together, the results of these long-term tumor studies suggest that silymarin affords substantial protection against photocarcinogenesis, and that the statistically not significant protective effect against tumor initiation is possibly due to low tumor incidence and tumor multiplicity in the control group.

Mouse skin has been a widely accepted model for studying photocarcinogenesis and for identifying the associated cellular, biochemical, and molecular events (*8,9,12,43,44*). With regard to UVB radiation-induced tumor initiation, it is known that UVB exposure results in DNA damage in epidermal cells, leading to the formation of cyclobutane dimers and 6-4 photoproducts (*20-24*). Some of this DNA damage is repaired by enzymatic pathways catalyzed by endonucleases [reviewed in (*20-24,28*)]. The unrepaired lesions lead to the fixation of mutation in the target genes, one of which is presumably the p53 tumor suppressor gene (*44-49*). Earlier (*50*), it had also been shown that the activation of ras oncogenes by point mutation plays a role in nonmelanoma human skin cancers. However, recently we have demonstrated that such genetic alterations are rare in photocarcinogenesis (*51*), which further supports a role for p53 in UV-

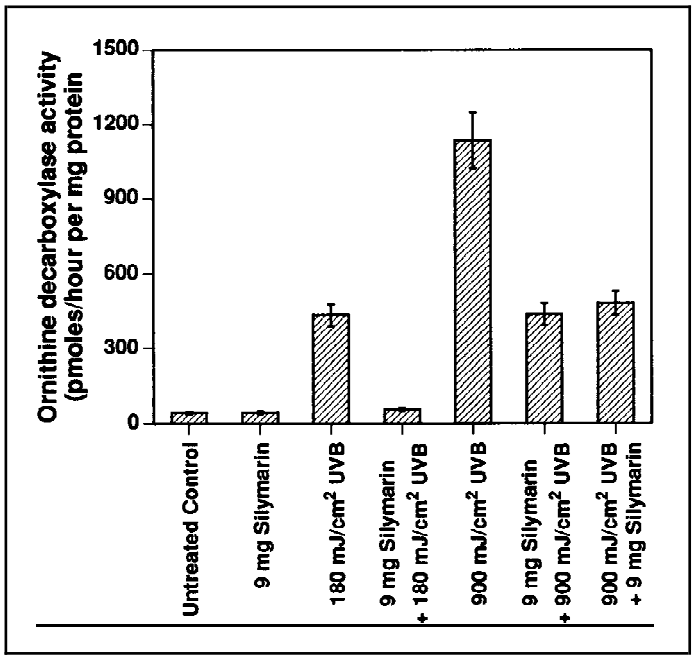

Fig. 7. Inhibitory effect of silymarin on UVB-caused induction of epidermal ornithine decarboxylase (ODC) activity in SKH-1 hairless mice. The groups of mice (four animals per group) were either unexposed (untreated control), treated topically on dorsal skin with silymarin (9 mg in 200 μL acetone per mouse), exposed to UVB radiation (180 mJ or 900 mJ per cm^2), with or without topical application of silymarin (9 mg in 200 μL acetone per mouse) 30 minutes prior to UVB radiation, or first exposed to UVB radiation (900 mJ/cm^2) and immediately thereafter treated topically with silymarin (9 mg in 200 μL acetone per mouse). Twenty-four hours after UVB irradiation, the animals were killed, epidermal cytosolic fraction was prepared, and ODC activity was determined. The data shown as ODC activity (picomoles per hour per milligram of protein) are mean ± standard error of four mice; each assay was performed in duplicate.

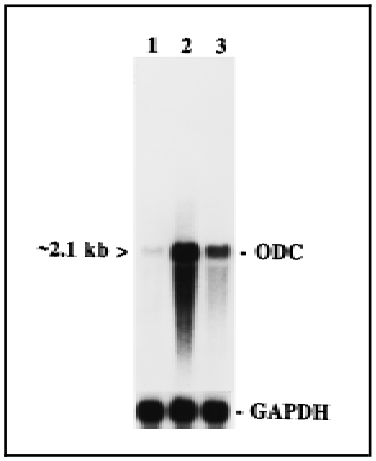

Fig. 8. Inhibitory effect of silymarin on UVB-caused induction of epidermal ornithine decarboxylase (ODC) messenger RNA expression in SKH-1 hairless mice. The groups of four mice each were either unexposed or exposed to UVB radiation (180 or 900 mJ/cm^2) with or without topical application of silymarin (9 mg in 200 μL acetone per mouse) 30 minutes prior to UVB exposure. Twenty-four hours after UVB irradiation, the animals were killed, and total RNA was isolated from the epidermis and poly(A)$^+$ RNA was purified using oligo(dT)-cellulose columns. The poly(A)$^+$ RNA samples were subjected to agarose gel electrophoresis, and separated poly(A)$^+$ RNA was transferred onto membrane by northern blotting and hybridized to the ^{32}P-labeled ODC complementary probe. Poly(A)$^+$ RNA samples from unexposed control epidermis (lane 1); UVB-irradiated epidermis (lane 2); and silymarin + UVB-irradiated epidermis (lane 3). In each case, 4 μg of poly(A)$^+$ RNA was loaded per lane. The same blot was stripped and rehybridized with a glyceraldehyde-3-phosphate dehydrogenase (GAPDH) probe.

caused genetic lesions. It has also been demonstrated that UVB irradiation results in sunburn and apoptotic cell formation in the epidermis of $p53^{+}/^{+}$ mice (wild-type) (*52*). Inactivating p53 in mouse skin by using $p53^{-}/^{-}$ mice (knockout), however, reduces the appearance of sunburn cells, the damaged keratinocytes generated by overexposure to UV (*52*). It has also been suggested that sunburn cells with a p53 mutation can be selected for clonal expansion into actinic keratosis (*52*,*53*), which is a preneoplastic condition for squamous cell carcinoma. These studies (*52*,*53*) suggest that the formation of cyclobutane dimers and 6-4 photoproducts followed by fixation of mutation in p53 and generation of sunburn and apoptotic cells are the sequential events that lead to UVB-caused tumor initiation. We have very recently shown that topical application of silymarin at the dose of 6 mg per mouse 30 minutes prior to UVB exposure at the dose of 1200 mJ/cm^2 resulted in a 63% reduction in the formation of cyclobutane pyrimidine dimers compared with animals that did not receive silymarin (*54*). The inhibitory effects of silymarin against UVB radiation-induced cyclobutane pyrimidine dimers (*54*) and sunburn cell and apoptotic cell formation (Fig. 4) in mouse epidermis clearly explain its protective effects against UVB-induced complete carcinogenesis observed in the present study (Fig. 3). The exact mechanism by which silymarin exerts its inhibitory effects against UVB radiation-induced formation of cyclobutane pyrimidine dimers, sunburn cells, and apoptotic cells in mouse epidermis is not clear at this point. Whereas most of the cellular DNA damage is due to the absorption of UV wavelength at 300 nm (*20*,*21*), the absorption spectrum of silymarin in methanol has a UV-absorption maximum at 288 nm (*55*). This suggests that silymarin is not shielding the absorption of UVB by cellular epidermal DNA.

We also performed studies to explore whether topical application of silymarin exerts its inhibitory effect by acting as a sunscreen. Silymarin (9 mg per mouse) was applied topically immediately after or 30 minutes prior to the UVB irradiation (900 mJ/cm^2), and effects on UVB-caused cutaneous edema and induction of COX and ODC activities were assessed. Comparable inhibitory effects of silymarin were observed in both experiments. Collectively, these observations suggest that the protective effects of silymarin reported in this study are not due to a sunscreen effect.

Unlike the tumor initiation process, UVB radiation-induced tumor promotion is associated with several cellular, biochemical, and molecular events. These include a generation of free radicals and ROS, depletion of antioxidant systems, acute inflammation characterized as skin edema, induction of COX activity, increased enzyme activity and mRNA expression of ODC, etc. (*25*-*29*,*35*,*39*). Although the sequence of these events is not established, it is largely agreed that oxidative stress is an important contributor (*25*-*29*,*35*,*39*). The significant inhibitory effect of silymarin against UVB-caused skin and ear edema (Fig. 5) suggests that strong antioxidant activity of silymarin may be responsible for the observed inhibition. Silymarin may scavenge UVB-generated ROS and free radicals by terminating biologic reactions that generate them and/or protecting the depletion of the antioxidant system. In in vitro studies, we found that the addition of silymarin to epidermal and hepatic microsomal suspension results in the significant inhibition of lipid peroxidation (data not shown) that supports the first possibility. We also observed a significant protection against UVB radiation-induced depletion of catalase activity (an antioxidant enzyme) by silymarin that supports the second possibility.

COX-mediated formation of PGs (specifically PGE_2) is another important event in UVB radiation-caused skin inflammation and tumor promotion (*35*). Arachidonic acid, released from skin phosphatidylcholine by the activation of skin phospholipase A_2 because of UVB exposure, undergoes oxidative metabolism involving the COX pathway, resulting in PG formation (*35*,*39*,*56*). The UVB-caused increase in epidermal COX activity observed in this study (Fig. 6) and reported earlier (*39*) further suggests its role in UVB-caused oxidative stress and tumor promotion. Similarly, induction of ODC activity and mRNA expression caused by UVB and other tumor promoters is considered to be an important event in tumor promotion (*35*-*39*). The significant inhibitory effects of silymarin against UVB-caused induction of epidermal COX activity (Fig. 6) and ODC activity (Fig. 7) and mRNA expression (Fig. 8) clearly explain its protective effects against UVB-caused tumor promotion and complete carcinogenesis (Fig. 3).

In summary, we have shown that silymarin, a naturally occurring flavonoid compound, exerts highly protective effects against photocarcinogenesis in the mouse skin model. On the basis of the results of the present study, clinical trials exploring the usefulness of silymarin as a protective agent against solar radiation-induced nonmelanoma skin cancers in humans are warranted.

References

(*1*) Miller DL, Weinstock MA. Nonmelanoma skin cancer in the United States: incidence. J Am Acad Dermatol 1994;30:774-8.

(*2*) Marks R. An overview of skin cancers. Incidence and causation. Cancer 1995;75(2 Suppl):607-12.

(*3*) Epstein JH. Photocarcinogenesis, skin cancer, and aging. In: Balin AK, Kligman AM, editors. Aging and the skin. New York: Raven Press, 1989: 307-46.

(*4*) Freeman RG. Action spectrum for ultraviolet carcinogenesis. Natl Cancer Inst Monogr 1978;50:27-9.

(*5*) Elmets CA, Mukhtar H. Ultraviolet radiation and skin cancer: progress in pathophysiologic mechanisms. Progr Dermatol 1996;30:1-16.

(*6*) van Weelden H, de Gruijl FR, van der Putte SC, Toonstra J, van der Leun JC. The carcinogenic risk of modern tanning equipment: is UV-A safer than UV-B? Arch Dermatol Res 1988;280:300-7.

(*7*) Sterenborg HJ, van der Leun JC. Tumorigenesis by a long wavelength UV-A source. Photochem Photobiol 1990;51:325-30.

(*8*) de Gruijl FR, Forbes PD. UV-induced skin cancer in a hairless mouse model. Bioessays 1995;17:651-60.

(*9*) Forbes PD. Relevance of animal models of photocarcinogenesis to humans. Photochem Photobiol 1996;63:357-62.

(*10*) Elmets CA, Anderson CY. Sunscreens and photocarcinogenesis: an objective assessment. Photochem Photobiol 1996;63:435-40.

(*11*) Wolf P, Donawho CK, Kripke ML. Effect of sunscreens on UV radiation-induced enhancement of melanoma growth in mice. J Natl Cancer Inst 1994;86:99-105.

(*12*) Agarwal R, Mukhtar H. Chemoprevention of photocarcinogenesis. Photochem Photobiol 1996;63:440-4.

(*13*) Ames BN, Gold LS, Willett WC. The causes and prevention of cancer. Proc Natl Acad Sci U S A 1995;92:5258-65.

(*14*) Boone CW, Kelloff GJ, Malone WE. Identification of candidate cancer chemopreventive agents and their evaluation in animal models and human clinical trials: a review. Cancer Res 1990;50:2-9.

(*15*) Wattenberg LW. Inhibition of carcinogenesis by naturally occurring and synthetic compounds. In: Kuroda Y, Shankel DM, Waters MD, editors. Antimutagenesis and anticarcinogenesis, mechanisms. II. New York: Plenum Publishing Corp, 1990:155-66.

(*16*) Black HS, Herd A, Goldberg LH, Wolf JE Jr, Thornby JI, Rosen T, et al. Effect of a low-fat diet on the incidence of actinic keratosis. N Engl J Med 1994;330:1272-5.
(*17*) Chen LC, De Luca LM. Retinoid effects on skin cancer. In: Mukhtar H, editor. Skin cancer: mechanism and human relevance. Boca Raton (FL): CRC Press, 1995:401-24.
(*18*) Al-Salem T, Ali ZS, Qassab M. Skin cancer in xeroderma pigmentosum: response to indomethacin and steroids [letter]. Lancet 1980;1:264-5.
(*19*) Vink AA, Yarosh DB, Kripke ML. Chromophore for UV-induced immunosuppression: DNA. Photochem Photobiol 1996;63:383-6.
(*20*) Chan GL, Peak MJ, Peak JG, Haseltine WA. Action spectrum for the formation of endonuclease-sensitive sites and (6-4) photoproducts induced in a DNA fragment by ultraviolet radiation. Int J Radiat Biol 1986;50: 641-8.
(*21*) Rosenstein BS, Mitchell DL. Action spectra for the induction of pyrimidine(6-4)pyrimidone photoproducts and cyclobutane pyrimidine dimers in normal human skin fibroblasts. Photochem Photobiol 1987;45:775-80.
(*22*) Protic-Sabljic M, Tuteja N, Munson PJ, Hauser J, Kraemer KM, Dixon K. UV light-induced cyclobutane pyrimidine dimers are mutagenic in mammalian cells. Mol Cell Biol 1986;6:3349-56.
(*23*) Hart RW, Setlow RB, Woodhead AD. Evidence that pyrimidine dimers in DNA can give rise to tumors. Proc Natl Acad Sci U S A 1977;74:5574-8.
(*24*) Mitchell DL, Nairn RS. The biology of the (6-4) photoproduct. Photochem Photobiol 1989;49:805-19.
(*25*) Pathak MA, Stratton K. Free radicals in human skin before and after exposure to light. Arch Biochem Biophys 1968;123:468-76.
(*26*) Taira J, Mimura K, Yoneya T, Hagi A, Murakami A, Makino K. Hydroxyl radical formation by UV-irradiated epidermal cells. J Biochem 1992;111: 693-5.
(*27*) Shindo Y, Witt E, Packer L. Antioxidant defense mechanisms in murine epidermis and dermis and their responses to ultraviolet light. J Invest Dermatol 1993;100:260-5.
(*28*) Mukhtar H, Elmets CA. Photocarcinogenesis: mechanisms, models and human health implications. Photochem Photobiol 1996;63:356-7.
(*29*) Tyrrell RM. Oxidant, antioxidant status and photocarcinogenesis: the role of gene activation. Photochem Photobiol 1996;63:380-3.
(*30*) Letteron P, Labbe G, Degott C, Berson A, Fromenty B, Delaforge M, et al. Mechanism for the protective effects of silymarin against carbon tetrachloride-induced lipid peroxidation and hepatotoxicity in mice. Evidence that silymarin acts both as an inhibitor of metabolic activation and as a chain-breaking antioxidant. Biochem Pharmacol 1990;39:2027-34.
(*31*) Mereish KA, Bunner DL, Ragland DR, Creasia DA. Protection against microcystin-LR-induced hepatotoxicity by Silymarin: biochemistry, histopathology, and lethality. Pharm Res 1991;8:273-7.
(*32*) Mourelle M, Muriel P, Favari L, Franco T. Prevention of CCl4-induced liver cirrhosis by silymarin. Fundam Clin Pharmacol 1989;3:183-91.
(*33*) Valenzuela A, Guerra R, Videla LA. Antioxidant properties of the flavonoids silybin and (+)-cyanidanol-3: comparison with butylated hydroxyanisole and butylated hydroxytoluene. Planta Med 1986;52:438-40.
(*34*) Comoglio A, Leonarduzzi G, Carini R, Busolin D, Basaga H, Albano E, et al. Studies on the antioxidant and free radical scavenging properties of IdB 1016: a new flavanolignan complex. Free Radic Res Commun 1990;11: 109-15.
(*35*) Agarwal R, Mukhtar H. Oxidative stress in skin chemical carcinogenesis. In: Packer L, Fuchs J, editors. Oxidative stress in dermatology. New York: Marcel Dekker Inc, 1993;207-41.
(*36*) Perchellet JP, Perchellet EM. Antioxidants and multistage carcinogenesis in mouse skin. Free Radic Biol Med 1989;7:377-408.
(*37*) O'Brien TG. The induction of ornithine decarboxylase as an early, possibly obligatory, event in mouse skin carcinogenesis. Cancer Res 1976;36:2644-53.
(*38*) Agarwal R, Katiyar SK, Lundgren DW, Mukhtar H. Inhibitory effect of silymarin, an anti-hepatotoxic flavonoid, on 12-*O*-tetradecanoylphorbol-13-acetate-induced epidermal ornithine decarboxylase activity and mRNA in SENCAR mice. Carcinogenesis 1994;15:1099-103.
(*39*) Agarwal R, Katiyar SK, Khan SG, Mukhtar H. Protection against ultraviolet B radiation-induced effects in the skin of SKH-1 hairless mice by a polyphenolic fraction isolated from green tea. Photochem Photobiol 1993; 58:695-700.
(*40*) Wang ZY, Huang MT, Ferraro T, Wong CQ, Lou YR, Iatropoulos M, et al. Inhibitory effect of green tea in the drinking water on tumorigenesis by ultraviolet light and 12-*O*-tetradecanoylphorbol-13-acetate in the skin of SKH-1 mice. Cancer Res 1992;52:1162-70.
(*41*) Wolf P, Cox P, Yarosh DB, Kripke ML. Sunscreens and T4N5 liposomes differ in their ability to protect against ultraviolet-induced sunburn cell formation, alterations of dendritic epidermal cells, and local suppression of contact hypersensitivity. J Invest Dermatol 1995;104:287-92.
(*42*) Mizuno N, Kono T, Tanii T, Ishii M, Hamada T, Yoshida H, et al. Increase in the expression of the ornithine decarboxylase gene in mouse skin by ultraviolet light. Arch Dermatol Res 1989;281:514-6.
(*43*) Kripke ML. Latency, histology, and antigenicity of tumors induced by ultraviolet light in three inbred mouse strains. Cancer Res 1977;37:1395-400.
(*44*) Kraemer KH. Sunlight and skin cancer: another link revealed. Proc Natl Acad Sci U S A 1997;94:11-4.
(*45*) Ziegler A, Jonason A, Simon J, Leffell D, Brash DE. Tumor suppressor gene mutations and photocarcinogenesis. Photochem Photobiol 1996;63:432-5.
(*46*) Nataraj AJ, Trent JC 2nd, Ananthaswamy HN. p53 gene mutations and photocarcinogenesis. Photochem Photobiol 1995;62:218-30.
(*47*) Brash DE, Rudolph JA, Simon JA, Lin A, McKenna GJ, Baden HP, et al. A role for sunlight in skin cancer: UV-induced p53 mutations in squamous cell carcinoma. Proc Natl Acad Sci U S A 1991;88:10124-8.
(*48*) Pierceall WE, Mukhopadhyay T, Goldberg LH, Ananthaswamy HN. Mutations in the p53 tumor suppressor gene in human cutaneous squamous cell carcinomas. Mol Carcinog 1991;4:445-9.
(*49*) Ziegler A, Leffell DJ, Kunala S, Sharma HW, Gailani M, Simon JA, et al. Mutation hotspots due to sunlight in the p53 gene of nonmelanoma skin cancers. Proc Natl Acad Sci U S A 1993;90:4216-20.
(*50*) Ananthaswamy HN, Pierceall WE. Molecular mechanisms of ultraviolet radiation carcinogenesis. Photochem Photobiol 1990;52:1119-36.
(*51*) Khan SG, Mohan RR, Katiyar SK, Wood GS, Bickers DR, Mukhtar H, et al. Mutations in ras oncogenes: rare events in ultraviolet B radiation-induced mouse skin tumorigenesis. Mol Carcinog 1996;15:96-103.
(*52*) Ziegler A, Jonason AS, Leffell DJ, Simon JA, Sharma HW, Kimmelman J, et al. Sunburn and p53 in the onset of skin cancer. Nature 1994;372:773-6.
(*53*) Jonason AS, Kunala S, Price GJ, Restifo RJ, Spinelli HM, Persing JA, et al. Frequent clones of p53-mutated keratinocytes in normal human skin. Proc Natl Acad Sci U S A 1996;93:14025-9.
(*54*) Chatterjee ML, Agarwal R, Mukhtar H. Ultraviolet B radiation-induced DNA lesions in mouse epidermis: an assessment using a novel 32P-postlabelling technique. Biochem Biophys Res Commun 1996;229:590-5.
(*55*) Wagner H, Horhammer L, Munster R. Chemistry of silymarin (silybin), the active principle of the fruits of *Silybum marianum* (*L.*) *Gaertn.* (*Carduus marianus L.*). Arzneimittelforschung 1968;18:688-96.
(*56*) Miller CC, Hale P, Pentland AP. Ultraviolet B injury increases prostaglandin synthesis through a tyrosine kinase-dependent pathway. Evidence for UVB-induced epidermal growth factor receptor activation. J Biol Chem 1994;269:3529-33.

Notes

Supported by Public Health Service grant CA64514 (R. Agarwal) from the National Cancer Institute, National Institutes of Health, Department of Health and Human Services.

We thank Dr. Saeid B. Amini, Department of Epidemiology and Biostatistics, School of Medicine, Case Western Reserve University, for his expert advice and assistance in the statistical analysis of the tumorigenesis data.

Manuscript received October 8, 1996; revised January 31, 1997; accepted February 13, 1997.